ISSN 1063-7788, Physics of Atomic Nuclei, 2021, Vol. 84, No. 2, pp. 207–211. © Pleiades Publishing, Ltd., 2021.
Russian Text © The Author(s), 2021, published in Yadernaya Fizika, 2021, Vol. 84, No. 2, pp. 166–170.

ELEMENTARY PARTICLES AND FIELDS
Experiment

Boron Neutron Capture Therapy

S. Yu. Taskaev[1),2)*]

Received April 13, 2020; revised April 13, 2020; accepted April 13, 2020

Abstract—Fundamentals of boron neutron capture therapy of malignant tumors are outlined, and the current status of the development of epithermal-neutron sources on the basis of charged-particle accelerators is surveyed. Attention is additionally given to a neutron source based on a charged-particle accelerator belonging to a new type—a tandem accelerator with vacuum insulation and a lithium neutron-producing target.

DOI: `10.1134/S106377882101021X`

According to World Health Organization data, cancer steadily becomes more frequent, leading to significant mortality. The development of drugs and methods for treating malignant tumors is an important and as-yet-unresolved scientific problem. Presently, boron neutron capture therapy (BNCT) is viewed as a promising approach in treating a number of malignant tumors, primarily hardly tractable brain tumors. This method is especially attractive owing to its selective effect on the cells of malignant tumors [1, 2].

The BNCT method is a binary-radiotherapy form that employs a uniquely high ability of a nonradioactive boron-10 nucleus to absorb a thermal neutron. The cross section for this absorption reaction is 3837 b. Neutron absorption by a ^{10}B nucleus initiates instantaneously the nuclear reaction $^{10}\mathrm{B}(n,\alpha)^7\mathrm{Li}$ accompanied by an energy deposition of 2.79 MeV. In 6.1% of cases, this energy is distributed only between a lithium nucleus and an alpha particle. In 93.9% of cases, the lithium nucleus escapes in an excited state and emits a photon of energy 0.48 MeV. The products of the nuclear reaction in question (lithium nucleus of energy 0.84 MeV and alpha particle of energy 1.47 MeV) are characterized by a high stopping power and by a short range in water or in body tissue—5.2 and 7.5 μm; this is commensurate with the size of mammalian cells. The stopping power for a photon is substantially lower. It follows that, in the nuclear reaction $^{10}\mathrm{B}(n,\alpha)^7\mathrm{Li}$, the energy is mostly deposited (specifically 84% of it) within a single cell. Thus, a selective accumulation of boron-10 within a tumor cell and a subsequent irradiation with neutrons should lead to the destruction of tumor cells but entail a relatively weak damage of surrounding normal cells.

The main requirement for a therapeutic neutron beam is as follows: the neutron flux density in the epithermal energy range (from 0.5 eV to 10 keV) should be higher than 10^9 cm^{-2} s^{-1}; in addition, the contribution of fast neutrons and gamma radiation to the absorbed dose should be less than 2×10^{-13} Gy cm^2 per epithermal neutron [3].

Clinical tests of the BNCT procedure were performed at nuclear reactors, and positive results were obtained in treating glioblastoma, melanoma, neck tumors, meningioma, pleural mesothelioma, and hepatocellular carcinoma [1].

A broad adaptation of this procedure in clinical practice is associated with the application of charged-particle accelerators owing to their safety and the possibility of obtaining therapeutic neutron beams of higher quality. Attention is given primarily to the following two threshold reactions: $^7\mathrm{Li}(p,n)^7\mathrm{Be}$ and $^9\mathrm{Be}(p,n)^9\mathrm{B}$; of these, the reaction $^7\mathrm{Li}(p,n)^7\mathrm{Be}$ is recognized to be the better one because of the maximum yield and the minimum neutron energy [4].

Several groups of researchers were able to solve the problem of creating an accelerator source of epithermal neutrons, and the first five BNCT clinical centers are presently under construction worldwide. They are constructed by different teams employing everywhere different technical solutions.

1. A 30-MeV 1-mA cyclotron and a beryllium target developed by the Japanese company Sumitomo Heavy Industries were mounted at the clinic in South Tohuku (Fukushima Prefecture, Japan). In March 2020, this team reported on getting a license to manufacture, exploit, and sell facilities of this type [5] and an approval to use steboronine [6], which is a new preparation for a targeted boron delivery (earlier,

---

[1)] Budker Institute of Nuclear Physics, Siberian Branch, Russian Academy of Sciences, Novosibirsk, Russia.

[2)] Novosibirsk State University, Novosibirsk, Russia.

[*] E-mail: `taskaev@inp.nsk.su`

boron phenylalanine and boron sulfhydryl were in use for this purpose in clinical tests at nuclear reactors).

2. The University of Tsukuba (Japan), together with Mitsubishi Heavy Industries, ltd., and the KEK and JAERI research institutions, produced and commissioned an 8-MeV 5-mA linear accelerator (linac) and a beryllium target. A proton beam of current 2.8 mA has been obtained to date.

3. The AccSys Technology, Inc. (USA), a subsidiary of Hitachi, manufactured a 2.5 MeV linac rated to a current of 20 mA for the National Oncological Center in Tokyo. A lithium target developed by the Linac Systems company is used to produce neutrons. A proton beam of current 11 mA has been obtained to date.

4. The Neutron Therapeutics company (USA) manufactured and commissioned a direct-action 2.6-MeV 30-mA electrostatic accelerator at the clinic of the University of Helsinki (Finland). A rotating lithium target is used to produce neutrons.

5. At the request of Neuboron Medtech (Nankin, China), the TAE Life Sciences company (California, USA) produced a 2.5-MeV 10-mA tandem accelerator and a lithium target for the clinic in Xiamen (China). The tandem accelerator with vacuum insulation and lithium target, proposed and developed (for more details, see below) at Budker Institute of Nuclear Physics (BINP, Siberian Branch, Russian Academy of Sciences) served as a prototype.

All five BNCT centers plan to begin curing patients in 2020. For a detailed description of the above technological solutions, the interested reader is referred to the monograph of Taskaev and Kanygin [2] and to the review article of Taskaev [7]; references to the original studies can also be found there.

A schematic diagram of the BINP accelerator-based neutron source is shown in Fig. 1.

A new type of charged-particle accelerators was proposed with aim of obtaining a steady-state proton beam of low energy [8]. Later, it was commonly called a vacuum-insulated tandem accelerator (*5*). The accelerator in question is a tandem. This means that, first, an electric field accelerates negative hydrogen ions, whereupon, after electrons are stripped off in a gas stripping target (*7*), the same field accelerates positive ions. In contrast to traditional tandem accelerators, no accelerator tubes are used in this version—the electrodes (*6*) are fastened to a single feedthrough insulator (*17*), as is shown in Fig. 1. This modification was proposed in order to implement the main idea of the new accelerator—to place the insulator as far as is possible from the accelerator channel with the aim of reducing the probability for charged secondaries and ultraviolet radiation originating from the interaction of beam ions with the residual and stripping gases to hit the insulator. This will permit increasing the proton-beam current.

The vacuum-insulated tandem accelerator is compact (it is 2 m height and 1.4 m in diameter); as a consequence, it provides a high ion-acceleration rate of up to 25 keV/cm; a wide range of ion energies—from 0.6 to 2.3 MeV; a wide current range—from 0.5 to 9 mA; high stability and monochromaticity of energy (0.1%); high current stability (0.5%); and the possibility of obtaining not only a proton beam but also a deuteron beam [9].

Special problems of the accelerator are associated with a large surface area of the electrodes and a high ion-acceleration rate. Because of a large electrode area, a large amount of energy is accumulated in accelerating gaps, so that, in order to prevent the reduction of their high-voltage breakdown strength, it is necessary to train the gaps with a dark current of limited magnitude. The manufacturing of the feedthrough insulator (*17*) from ceramic rings with a corrugated outer surface made it possible to get rid of a breakdown along the vacuum surface of the insulator and to ensure a stable production of the proton beam. Because of a high ion-acceleration rate, the inlet electrostatic lens is strong. This requires refocusing the injected beam of negative hydrogen ions in front of the inlet lens of the accelerator. The controlled injection of the ion beam under the effect of the space charge in the transportation channel is ensured by a wire scanner (*3*) positioned in front of the inlet diaphragm of the accelerator (*4*) [10].

Flows of secondary charged particles were found in the accelerator. They were due to ionization induced by the beams of ions of the residual and stripping gases, the penetration of electrons from the transportation channel to accelerating gaps, and electron emission from the vacuum-tank walls irradiated with positively charged secondary ions. Owing to placing, at the inlet of the accelerator, a cooled diaphragm, a ring at a negative potential, and an additional vacuum pump and to coating part of vacuum-tank walls with a metal grid at a negative potential, it became possible to attain a nearly tenfold suppression of the current of charged secondaries in the accelerating gaps: from initial 60% of the ion-beam current to a level below 8% [11].

At the same time, ionization induced by the beam of ions of the residual and stripping gases generates radiation in the visible spectrum and makes it possible to visualize it. This is used to monitor the position and size of the ion beam.

The beam-transportation channel is used to deliver the proton beam to the neutron-producing target. This channel is equipped with a corrector (*11*) for guiding the proton beam, a bending magnet (*12*)

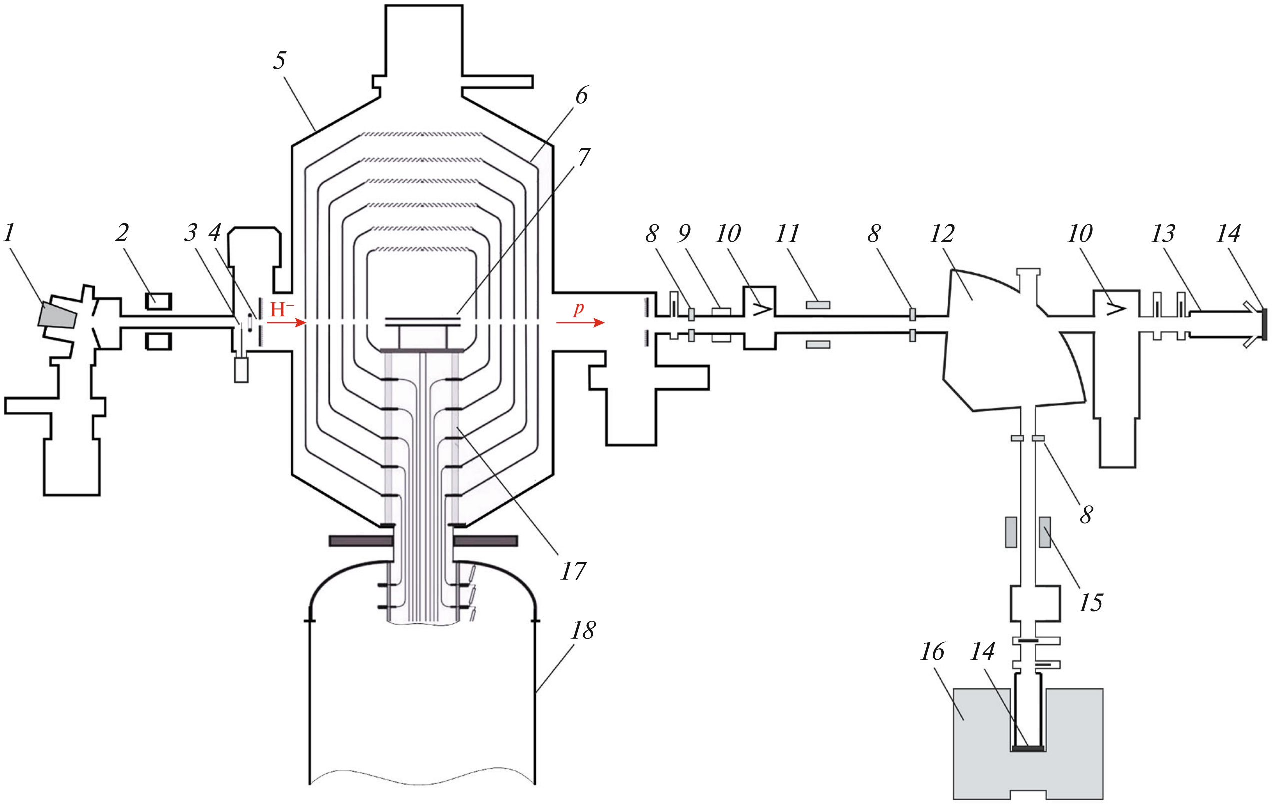

Fig. 1. Accelerator-based neutron source: (*1*) source of negative hydrogen ions, H^-; (*2*) magnetic lens; (*3*) wire scanner; (*4*) inlet cooled diaphragm of the accelerator; (*5*) vacuum-insulated tandem accelerator; (*6*) electrodes; (*7*) gas stripping target; (*8*) cooled copper diaphragms; (*9*) noncontact current transformer; (*10*) pullout Faraday cup; (*11*) corrector; (*12*) bending magnet, (*13*) target unit; (*14*) lithium target; (*15*) scanner; (*16*) neutron-beam shaping assembly, (*17*) feedthrough insulator; and (*18*) high-voltage sectioned rectifier. The arrows indicate the directions of propagation of negative hydrogen ions (H^-) and protons (p).

for rotating the proton beam downward through an angle of 90°, a scanner (*15*) for sweeping the target surface with the proton beam, three cooled copper diaphragms (*8*) with thermo couples for measuring the proton-beam position and for preventing the beam-induced burning-through of the vacuum chamber, two pullout Faraday cups (*10*) for monitoring the proton-beam current and position, and a noncontact current transformer (*9*) of the Bergoz (Bergoz Instr., France) NPCT (New Parametric Current Transformer) type (NPCT-CF4) for continuously measuring the proton-beam current. A target (*14*) is used for the production of a neutron beam for BNCT in the vertical part of the channel and for other applications in its horizontal part.

Neutrons are produced as the result of the threshold reaction $^7\mathrm{Li}(p,n)^7\mathrm{Be}$. The lithium target (*14*) has three layers: a thin pure-lithium layer of crystal density formed by means of thermal vacuum deposition [12] and used for neutron production; a thin layer of a material that is resistant to radiation-induced blistering and which serves for proton absorption, and a thin copper substrate for efficient heat removal [13]. This simple target ensures the minimum possible level of undesirable accompanying gamma radiation and has an unprecedentedly long working lifespan.

The suppression of gamma radiation from the reaction $^7\mathrm{Li}(p,p'\gamma)^7\mathrm{Li}$ is achieved by choosing the lithium-layer thickness to be equal to the range of protons with initial energies of up to 1.882 MeV, which is the threshold for the reaction $^7\mathrm{Li}(p,n)^7\mathrm{Be}$. The results obtained at the beginning of 2020 with this facility for the $^7\mathrm{Li}(p,p'\gamma)^7\mathrm{Li}$ cross section and for the yield of gamma rays from a thick lithium target at proton energies between 0.7 and 1.85 MeV have a precision and reliability higher than those of the data presented in the literature and in the EXFOR database.

The unprecedentedly long working lifespan of the target was due to properly choosing the material of the second layer after performing in-situ observations of blistering of metallic samples exposed to a proton beam [14] and the respective observation of the target with a lithium layer. For the first time, we have proven experimentally that, in the created target, radiation-induced blistering does not lead to the reduction of the neutron yield. This fact changes the prevalent opinion on the impact of blistering on the working lifespan of the target and permits extending it, which is of importance for radiation therapy in clinics.

A beam shaping assembly that consists of a moderator, a reflector, an absorber, and filters is used to obtain a therapeutic neutron beam for BNCT at accelerator-based neutron sources. The neutron beam shaping assembly that we developed (*16* in Fig. 1) employs magnesium fluoride as a moderator and a composite reflector: graphite and lead, in respectively, the forward and backward hemispheres. By means of a numerical simulation of neutron and gamma-radiation transport, it was shown that a therapeutic neutron beam meeting the BNCT requirements to the maximum possible degree can be formed on the basis of the proposed solution at a proton energy of 2.3 MeV [15, 16].

Studies performed with the aid of the constructed facility revealed that neutron irradiation of tumor cells of human glioma U251 and human glioblastoma T98G that were preliminarily incubated in a boron-containing medium suppresses substantially their viability [17, 18]. The irradiation of mice in which a human glioblastoma tumor was implanted and in which boron phenylalanine enriched in the isotope ^{10}B was preliminarily introduced leads to their complete recovery [19].

The following promising studies are being performed at this facility: (i) A new method that consists in tagging a targeted-delivery preparation with an atomic nucleus activated under the effect of neutrons is proposed for dose measurements. (ii) In order to reduce the size of the neutron source and to ensure a better stability of the potential of the intermediate electrodes of the accelerator, the location of the lower part of the feedthrough insulator within the high-voltage sectioned rectifier was proposed [20] and was implemented in the facility manufactured for China. (iii) A neutron beam shaping assembly in which the neutron beam is orthogonal to the proton beam is proposed. The possibility rotating the beam shaping assembly or its part containing the moderator with respect to the proton-beam axis permits directing neutrons to the patient at an angle chosen in such a way as to reach the maximum effect of therapy for each specific tumor [21]. (iv) A neutron detector featuring a boron-enriched polystyrene scintillator was developed for measuring the “boron” dose [22]. (v) A method for obtaining a beam of neutrons that have energies within the epithermal range exclusively was developed and implemented with the aim of boron imaging by means of gamma spectroscopy.

The neutron source was used to measure the concentration of hazardous impurities in boron carbide samples manufactured for International Thermonuclear Experimental Reactor (ITER) [23] and is planned to be used for radiation test of optical cables in the system of laser calibration of the upgraded CMS electromagnetic detector for experiments at the Large Hadron Collider (CERN) in the high-luminosity mode [9]. The created facility involving specialized targets makes it possible to generate monochromatic and resonance gamma rays for developing a procedure for immediately finding explosive substances [24], alpha particles for studying the promising neutronless fusion reaction $^{11}\mathrm{B}(p,\alpha)\alpha\alpha$, and positrons in the reaction $^{19}\mathrm{F}(p,\alpha e^{+}e^{-})^{16}\mathrm{O}$.

CONCLUSIONS

Boron neutron capture therapy, which is very attractive because of its selective direct action on tumor cells, is considered as a promising method for treatment of many malignant tumors, especially incurable brain tumors. It is expected that treatment of patients will begin at the five BNCT clinics equipped with accelerator-based sources of epithermal neutrons. The vacuum-insulated tandem accelerator and the lithium target that were developed at BINP became a prototype of one of such sources. A steady-state proton beam of energy up to 2.3 MeV and current up to 9 mA was obtained at this accelerator, and a stable production of neutrons appropriate for BNCT was provided with the aid of the lithium target.

FUNDING

This work was sponsored by Russian Science Foundation (project no. 19-72-30005) and was supported by Budker Institute of Nuclear Physics, Siberian Branch, Russian Academy of Sciences.

REFERENCES

1. *Neutron Capture Therapy: Principles and Applications*, Ed. by W. Sauerwein, A. Wittig, R. Moss, and Y. Nakagawa (Springer, Berlin, 2012).
2. S. Yu. Taskaev and V. V. Kanygin, *Boron Neutron Capture Therapy* (SO RAN, Novosibirsk, 2016) [in Russian].
3. *Current Status of Neutron Capture Therapy,* IAEA-TECDOC-1223 (Vienna, Austria, 2001).
4. T. Blue and J. Yanch, J. Neuro-Oncol. **62**, 19 (2003).
5. https://www.shi.co.jp/english/info/2019/6kgpsq0000002ji0.html.
6. https://stella-pharma.co.jp/cp-bin/wordpress5/wp-content/uploads/2020/03/Press-release_Steboronine-approvalENG.pdf.
7. S. Yu. Taskaev, Phys. Part. Nucl. **46**, 956 (2015).

8. B. F. Bayanov, V. P. Belov, E. D. Bender, M. V. Bokhovko, G. I. Dimova, V. N. Kononov, O. E. Kononov, N. K. Kuksanov, V. E. Palchikov, V. A. Pivovarov, R. A. Salimov, G. I. Silvestrov, A. N. Skrinsky, N. A. Soloviov, and S. Yu. Taskaev, Nucl. Instrum. Methods Phys. Res., Sect. A **413**, 397 (1998).
9. D. A. Kasatov, A. M. Koshkarev, A. N. Makarov, G. M. Ostreinov, S. Yu. Taskaev, and I. M. Shchudlo, Instrum. Exper. Techn. **63**, 611 (2020).
10. T. A. Bykov, D. A. Kasatov, Ia. A. Kolesnikov, A. M. Koshkarev, A. N. Makarov, Yu. M. Ostreinov, E. O.'Sokolova, I. N. Sorokin, S. Yu. Taskaev, and I. M. Shchudlo, Instrum. Exp. Tech. **61**, 713 (2018).
11. A. Ivanov, D. Kasatov, A. Koshkarev, A. Makarov, Yu. Ostreinov, I. Shchudlo, I. Sorokin, and S. Taskaev, J. Instrum. **11**, P04018 (2016).
12. B. F. Bayanov, E. V. Zhurov, and S. Yu. Taskaev, Instrum. Exp. Tech. **51**, 147 (2008).
13. B. Bayanov, V. Belov, and S. Taskaev, J. Phys.: Conf. Ser. **41**, 460 (2006).
14. A. Badrutdinov, T. Bykov, S. Gromilov, Y. Higashi, D. Kasatov, I. Kolesnikov, A. Koshkarev, A. Makarov, T. Miyazawa, I. Shchudlo, E. Sokolova, H. Sugawara, and S. Taskaev, Metals **7**, 558 (2017).
15. L. Zaidi, E. A. Kashaeva, S. I. Lezhnin, G. N. Malyshkin, S. I. Samarin, T. V. Sycheva, S. Yu. Taskaev, and S. A. Frolov, Phys. At. Nucl. **80**, 60 (2017).
16. L. Zaidi, M. Belgaid, S. Taskaev, and R. Khelifi, Appl. Radiat. Isot. **139**, 316 (2018).
17. A. Zaboronok, V. A. Byvaltsev, V. V. Kanygin, A. I. Iarullina, A. I. Kichigin, A. V. Taranin, O. Yu. Volkova, L. V. Mechetina, S. Yu. Taskaev, R. A. Muhamadiyarov, E. L. Zavyalov, K. Nakai, E. Sato, T. Yamamoto, B. J. Mathis, and A. Matsumura, New Armen. Med. J. **11**, 6 (2017).
18. E. Sato, A. Zaboronok, T. Yamamoto, K. Nakai, S. Taskaev, O. Volkova, L. Mechetina, A. Taranin, V. Kanygin, T. Isobe, B. Mathis, and A. Matsumura, J. Radiat. Res. **59**, 101 (2018).
19. S. Yu. Taskaev, Phys. Part. Nucl. **50**, 569 (2019).
20. E. V. Domarov, A. A. Ivanov, N. K. Kuksanov, R. A. Salimov, I. N. Sorokin, S. Yu. Taskaev, and V. G. Cherepkov, Instrum. Exp. Tech. **60**, 70 (2017).
21. V. Aleynik, A. Bashkirtsev, V. Kanygin, D. Kasatov, A. Kuznetsov, A. Makarov, I. Schudlo, I. Sorokin, S. Taskaev, and M. Tiunov, Appl. Radiat. Isot. **88**, 177 (2014).
22. T. Bykov, D. A. Kasatov, A. M. Koshkarev, A. N. Makarov, V. V. Porosev, G. A. Savinov, I. M. Shchudlo, and S. Y. Taskaev, J. Instrum. **14**, P12002 (2019).
23. A. Shoshin, A. Burdakov, M. Ivantsivskiy, S. Polosatkin, M. Klimenko, A. Semenov, S. Taskaev, D. Kasatov, I. Shchudlo, A. Makarov, and N. Davydov, IEEE Trans. Plasma Sci. **48**, 1474 (2020).
24. A. Kuznetsov, Yu. I. Belchenko, A. V. Burdakov, V. I. Davydenko, A. S. Donin, A. A. Ivanov, S. G. Konstantinov, A. S. Krivenko, A. M. Kudryavtsev, K. I. Mekler, A. L. Sanin, I. N. Sorokin, Yu. S. Sulyaev, S. Yu. Taskaev, V. V. Shirokov, and Yu. I. Eidelman, Nucl. Instrum. Methods Phys. Res., Sect. A **606**, 238 (2009).